Cdc14-regulated midzone assembly controls anaphase B

Anton Khmelinskii,[1] Clare Lawrence,[2] Johanna Roostalu,[1] and Elmar Schiebel[1]

[1]Zentrum für Molekulare Biologie der Universität Heidelberg, 69120 Heidelberg, Germany
[2]The Paterson Institute for Cancer Research, Manchester M20 4BX, England, UK

Spindle elongation in anaphase of mitosis is a cell cycle–regulated process that requires coordination between polymerization, cross-linking, and sliding of microtubules (MTs). Proteins that assemble at the spindle midzone may be important for this process. In this study, we show that Ase1 and the separase–Slk19 complex drive midzone assembly in yeast. Whereas the conserved MT-bundling protein Ase1 establishes a midzone, separase–Slk19 is required to focus and center midzone components. An important step leading to spindle midzone assembly is the dephosphorylation of Ase1 by the protein phosphatase Cdc14 at the beginning of anaphase. Failure to dephosphorylate Ase1 delocalizes midzone proteins and delays the second, slower phase of anaphase B. In contrast, in cells expressing nonphosphorylated Ase1, anaphase spindle extension is faster, and spindles frequently break. Cdc14 also controls the separase–Slk19 complex indirectly via the Aurora B kinase. Thus, Cdc14 regulates spindle midzone assembly and function directly through Ase1 and indirectly via the separase–Slk19 complex.

Introduction

The spindle of eukaryotic cells is a complex microtubule (MT)-based machine that segregates chromosomes in mitosis and meiosis. Shortly before or at the beginning of mitosis, spindle MTs are nucleated from tubulin subunits either at the MT-organizing center or near chromatin (Carazo-Salas et al., 1999). The MT-organizing center is known as the centrosome in higher eukaryotes or as the spindle pole body (SPB) in yeast. The MTs then assemble through the action of MT-associated proteins into a bipolar spindle.

The mitotic spindle contains two distinct sets of MTs: the pole–kinetochore and the pole–pole MTs. The minus ends of both groups of MTs reside at the SPBs. The pole–kinetochore MTs interact at their plus end with kinetochores and move chromosomes to the spindle poles (anaphase A). The pole–pole MTs interdigitate in the middle of the spindle, thereby defining a spatially restricted region known as the central spindle or spindle midzone, and segregate chromosomes by elongating the spindle (anaphase B).

The properties of MTs change dramatically as cells transit the cell cycle. Through the rise of cyclin-dependent kinase (Cdk) activity, MT turnover increases as cells enter metaphase of mitosis (Belmont et al., 1990; Verde et al., 1990). Increased MT dynamics helps to reorganize the MT cytoskeleton into a bipolar spindle and promotes chromosome capture by kinetochore MTs (Cassimeris et al., 1994). With anaphase onset, MTs suddenly become stabilized (Mallavarapu et al., 1999; Pereira and Schiebel, 2003; Higuchi and Uhlmann, 2005). This is the combined result of decreased Cdk activity and the activation of protein phosphatases. A protein phosphatase that has been implicated in the regulation of anaphase spindle properties is the conserved Cdc14 (Pereira and Schiebel, 2003; Higuchi and Uhlmann, 2005). Cdc14 is involved in the dephosphorylation of spindle-associated proteins such as the DASH component Ask1 (Higuchi and Uhlmann, 2005) and directly regulates MT-binding activity of the inner centromere protein–Aurora B complex (Sli15-Ipl1 in yeast), which then, in turn, controls spindle localization of the chromosomal passenger protein Slk19 (Pereira and Schiebel, 2003).

An additional level of complexity arises from the targeting of a subset of spindle-associated proteins such as the MT-bundling protein Ase1, the Aurora B kinase complex, kinesin motor proteins, and, in yeast, the chromosomal passenger proteins Slk19 and separase Esp1 to the spindle midzone at the beginning of anaphase, where they participate in anaphase spindle formation and stabilization (Cooke et al., 1987; Zeng et al., 1999; Jensen et al., 2001; Mollinari et al., 2002; Schuyler et al., 2003).

A. Khmelinskii and C. Lawrence contributed equally to this paper.

Correspondence to Elmar Schiebel: e.schiebel@zmbh.uni-heidelberg.de

Abbreviations used in this paper: APC, anaphase-promoting complex; Cdk, cyclin-dependent kinase; MT, microtubule; SPB, spindle pole body; tdTomato, tandem-dimer Tomato; WT, wild type.

The online version of this article contains supplemental material.

The Journal of Cell Biology, Vol. 177, No. 6, June 18, 2007 981–993
http://www.jcb.org/cgi/doi/10.1083/jcb.200702145

Ase1 belongs to a functionally conserved family of MT-associated proteins (Schuyler et al., 2003) named Ase1 in fission yeast (Loiodice et al., 2005; Yamashita et al., 2005), Feo in *Drosophila melanogaster* (Verni et al., 2004), PRC1 in human cells (Jiang et al., 1998), SPD-1 in *Caenorhabditis elegans* (Verbrugghe and White, 2004), and MAP65 in plant cells (Chan et al., 1999). Although the degree of sequence identity is low, all family members bundle MTs, display specific midzone localization, and participate in anaphase spindle stability and cytokinesis (Juang et al., 1997; Mollinari et al., 2002; Schuyler et al., 2003; Balasubramanian et al., 2004; Norden et al., 2006). For example, human cells depleted of PRC1 by siRNA or yeast *ase1Δ* cells assemble a bipolar spindle, but severe defects in spindle morphology and function arise upon passage into anaphase (Juang et al., 1997; Mollinari et al., 2002; Loiodice et al., 2005; Zhu et al., 2006).

The ability of Ase1 to preferentially bundle antiparallel MT arrays makes it a key player in spindle midzone assembly (Janson et al., 2007). However, the cell cycle signals that target Ase1 to the spindle midzone at the beginning of anaphase and the identity of the proteins that cooperate with Ase1 in midzone assembly are barely understood. To identify proteins involved in these processes, we performed a systematic analysis of spindle midzone components in the model organism budding yeast. We show that Ase1 acts together with the separase–Slk19 complex to establish a functional spindle midzone independently of MT-based motor proteins. Cdc14 directly regulates spindle midzone assembly through the dephosphorylation of Ase1 and influences midzone centering indirectly via the separase–Slk19 complex. Phosphorylation of Ase1 in metaphase prevents the hyperactivation of spindle extension and spindle breakage during anaphase. Failure to dephosphorylate Ase1 with anaphase onset results in the delocalization of spindle midzone proteins along the entire length of the anaphase spindle and impairs the second, slower phase of anaphase spindle extension.

Results

Stepwise binding of Ase1, Slk19, Esp1, and Bim1 to the midzone of anaphase cells

The spindle midzone of budding yeast contains the MT-bundling protein Ase1 (Schuyler et al., 2003), separase Esp1 (Jensen et al., 2001), the Esp1 interactor Slk19 (Zeng et al., 1999; Sullivan and Uhlmann, 2003), the MT plus end–binding proteins Bim1 and Bik1 (Berlin et al., 1990; Schwartz et al., 1997), the Cin8 and Kip3 kinesin-like motor proteins (Saunders and Hoyt, 1992; DeZwaan et al., 1997), and the CLIP-associating protein–like molecule Stu1 (Yin et al., 2002). Some of these proteins (Ase1, Bik1, Bim1, Cin8, Kip3, and Stu1) are already associated with the metaphase spindle and become focused into a discrete zone between the two spindle poles with anaphase onset. In contrast, Esp1 and Slk19 are only recruited to the spindle after the onset of anaphase. We may expect that proteins that perform a leading function in spindle midzone assembly bind earlier than others that execute a more assisting role.

To gain insight into the formation of a functional spindle midzone, we compared the timing with which Ase1 associated with the spindle midzone to that of Bim1 and Slk19 association by time-lapse microscopy (Fig. 1 and Videos 1 and 2, available at http://www.jcb.org/cgi/content/full/jcb.200702145/DC1). We first analyzed the behavior of Ase1 and Slk19 using cells in which the chromosomal copy of *ASE1* was fused to GFP (*ASE1-GFP*) and *SLK19* was fused to the red fluorescent tandem-dimer Tomato ([tdTomato] *SLK19-tdTomato*). The *ASE1-GFP* and *SLK19-tdTomato* gene fusions were functional, as the elongated anaphase spindles of *cdc15-1 ASE1-GFP SLK19-tdTomato* cells were stable (unpublished data and Sullivan et al., 2001). We confirmed that Ase1 was already bound to the short spindle of preanaphase cells (Fig. 1 A, t = 0; Schuyler et al., 2003). In these cells, Slk19 associated with kinetochores, which, in yeast, cluster close to the SPBs (Jin et al., 1998). With anaphase onset, Ase1 accumulated at the spindle midzone between the two poles marked by the Slk19-tdTomato kinetochore signal (Fig. 1 A, 1 min 40 s; arrow). Slk19 localized slightly later than Ase1 to the emerging spindle midzone (Fig. 1 A, 2 min 30 s). Moreover, Slk19 left the spindle at the end of anaphase before Ase1 (Fig. 1 A, 15 min 0 s). These data were confirmed using still images of synchronized cells (Fig. S1). Thus, Ase1 binds to the assembling spindle midzone before Slk19.

Analysis of *ASE1-GFP BIM1-eqFP* cells (*BIM1* fused to the red fluorescent eqFP611 from the sea anemone *Entacmaea quadricolor*; Figs. 1 B and S1; Wiedenmann et al., 2002) showed that Bim1 associated with the spindle midzone with kinetics identical to Ase1.

Next, the spindle localization of Esp1 and Slk19 was determined in *ESP1-GFP SLK19-tdTomato* cells, in which the integrated *ESP1-GFP* was expressed from the native promoter. Because time-lapse analysis was challenging as a result of the weak Esp1-GFP signal, the localization of Esp1 and Slk19 was determined in still images (z stacks) of α-factor synchronized cells. The Esp1-GFP signal appeared with anaphase onset at both spindle poles, where it colocalized with Slk19-tdTomato (Fig. 1 C, i; arrowheads). When the spindle length was between 2 and 6 μm, Esp1 and Slk19 also colocalized at the spindle midzone (Fig. 1, C, ii; and D). Surprisingly, Esp1 left the spindle midzone before Slk19 (Fig. 1, C, iii; and D, >6 μm). Thus, Esp1 and Slk19 probably bind to the developing spindle midzone as a complex (Esp1–Slk19 complex formation has been demonstrated previously; Sullivan and Uhlmann, 2003) but later dissociate from the midzone with distinct kinetics. The notion that Esp1 and Slk19 bind as a complex was further supported by the finding of the interdependency of the spindle midzone binding of Esp1 and Slk19 (Fig. S2, available at http://www.jcb.org/cgi/content/full/jcb.200702145/DC1). Collectively, proteins bind to and leave the spindle midzone in a defined order, indicating a cell cycle–controlled program of spindle midzone assembly and disassembly.

Interdependency of the spindle midzone localization of Ase1 and Esp1–Slk19

Ase1 by itself or together with other proteins may function as a landmark for spindle midzone assembly to which other spindle midzone proteins bind either simultaneously or later than Ase1. To test this model, we analyzed the interdependency of the

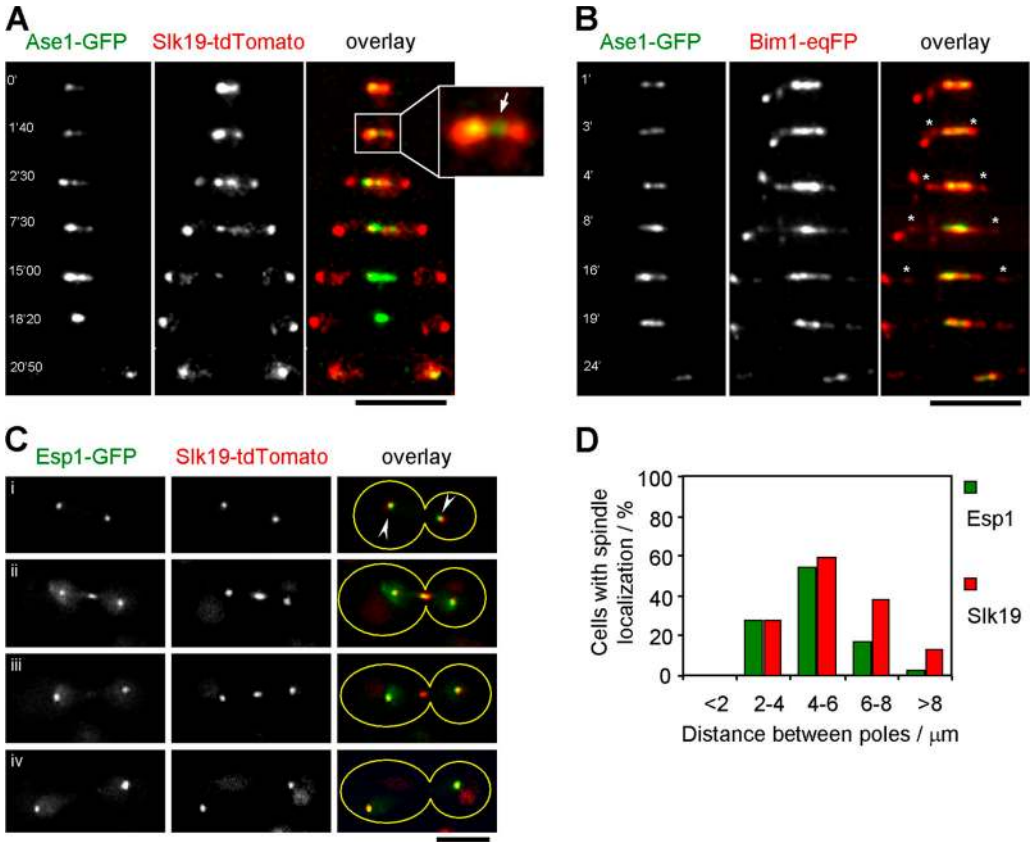

Figure 1. **Spindle binding of midzone components.** (A and B) *ASE1-GFP SLK19-tdTomato* (A) and *ASE1-GFP BIM1-eqFP* (B) cells were analyzed by time-lapse microscopy. Selected frames (maximum z-series projections) are shown. Time after the beginning of image acquisition is indicated in minutes. The inset in A is a magnification of the extending anaphase spindle of the *ASE1-GFP SLK19-tdTomato* cell. The arrow points toward Ase1 at the spindle center. (B) Asterisks mark spindle poles. (C) Analysis of α-factor synchronized *ESP1-GFP SLK19-tdTomato* cells. Early (i), mid- (ii), and late (iii–iv) anaphase cells. Arrowheads point to spindle poles. (D) Quantification of C. Approximate cell morphologies are indicated by yellow outlines drawn onto the overlaid images. Bars, 5 μm.

localization of spindle midzone proteins. Slk19 localization was analyzed in *mCherry-TUB1 SLK19-GFP* cells in the presence and absence of *ASE1* (Fig. 2 A). *mCherry-TUB1* enabled the visualization of the red fluorescent spindle. Cells were synchronized with α factor in G1 phase of the cell cycle (t = 0). Around 40–60 min after release from the G1 block, a short bipolar preanaphase spindle of similar length assembled in *ASE1* and *ase1*Δ cells (Fig. 2 B). At ∼60–80 min, *ASE1* and *ase1*Δ cells entered anaphase, as indicated by the increase in the proportion of large-budded cells and spindle elongation (Fig. 2 B). In *ASE1* wild-type (WT) cells, Slk19 associated with the midzone of spindles of intermediate length (3–8 μm; Fig. 2, A and B; red dots). In contrast, the anaphase spindles of *ase1*Δ cells were always devoid of Slk19 (Fig. 2, A and B). The reduced spindle length of *ase1*Δ cells did not account for this defect because the anaphase spindles of *ase1*Δ cells exceeded the 3-μm threshold after which Slk19 associates with spindles in WT cells (Figs. 1 A and 2 B). The spindle pole localization of Slk19 was not affected by the deletion of *ASE1*. Similar data were obtained for Esp1-GFP (Fig. S2). Thus, the Esp1–Slk19 complex requires the Ase1 protein or an Ase1-dependent structure for binding to the spindle midzone.

We next tested whether the Esp1–Slk19 complex controls the spindle localization of Ase1. This analysis was performed with *slk19*Δ cells carrying *ASE1-GFP mCherry-TUB1 SPC42-eqFP*. *SPC42-eqFP* allowed the unequivocal localization of the SPBs. In *slk19*Δ cells, as in WT cells, Ase1 bound only to a section of the anaphase spindle (Fig. 2 C). However, the Ase1-GFP zone of *slk19*Δ cells was more extended than in WT cells (Fig. 2 D). In addition, in 22% of *slk19*Δ cells, the Ase1-GFP signal was shifted toward one of the spindle poles (Fig. 2 C). A similar mislocalization of Ase1 was observed in conditional lethal *esp1-1* cells (Fig. S2; Sullivan et al., 2001). Together, these data indicate that the Esp1–Slk19 complex is important for both the spatial restriction and the centered localization of the spindle midzone protein Ase1.

Further analysis of the interdependency of spindle proteins showed that all midzone components (Bik1, Bim1, Cin8, Kip3, and Stu1) required the Ase1 landmark for recruitment to the spindle midzone and the Slk19 protein for spatial constraint to a centered spindle domain once recruited there by Ase1 (Fig. S3, available at http://www.jcb.org/cgi/content/full/jcb.200702145/DC1). In the absence of *SLK19*, these spindle midzone components frequently formed spatially restricted, albeit not centered, spindle domains. On the other hand, the deletion of *ASE1* abolished domain formation with the proteins binding uniformly along the interpolar MTs (Fig. S3). In contrast, the localization of other spindle components that evenly decorate WT anaphase

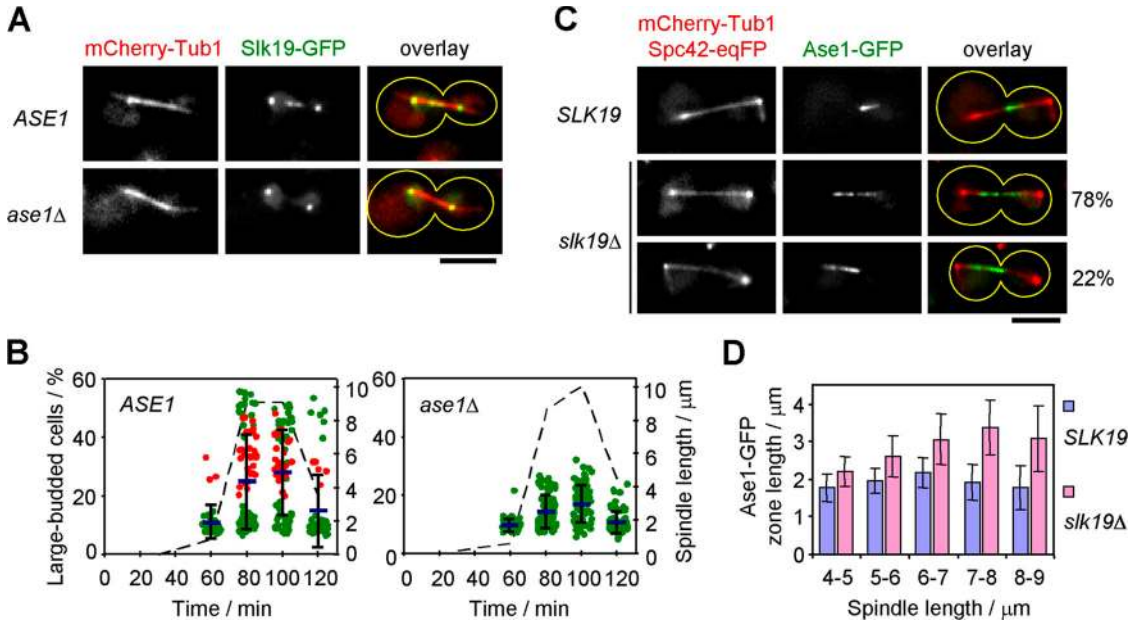

Figure 2. **Spindle midzone localization of Slk19 and Ase1 is interdependent.** (A and B) Slk19-GFP localization in *SLK19*-GFP *mCherry-TUB1* cells with and without *ASE1* synchronized with α factor (G1; t = 0). (B) Cells were analyzed at each time point for large buds (dotted lines), spindle length, and Slk19-GFP localization at the spindle midzone and poles (red dots) or only at the spindle poles (green dots). The mean spindle length (blue lines) with SD (error bars; black bars) is indicated for each time point. $n > 50$ per time point. (C and D) Ase1-GFP localization in *ASE1-GFP mCherry-TUB1 SPC42-eqFP* cells with and without *SLK19*. (C) The percentage of anaphase cells with centered or mislocalized Ase1-GFP spindle signal is shown on the right side of the figure. (D) Quantification of C. Mean value of the Ase1-GFP zone length with SD is shown for each spindle class. $n > 30$ per spindle class. Approximate cell morphologies are indicated by yellow outlines drawn onto the overlaid images. Bars, 5 μm.

spindles, such as Sli15, Ipl1, or Ndc10 (Bouck and Bloom, 2005; Norden et al., 2006), was not affected by the deletion of either *ASE1* or *SLK19* (Fig. S3). Thus, only the localization of spindle midzone proteins is dependent on Ase1 and the Esp1–Slk19 complex.

Finally, we asked whether the inactivation of other spindle components (*BIK1*, *BIM1*, *CIN8*, *FIN1*, *IPL1*, *KAR3*, *KIP1*, *KIP2*, *KIP3*, *NDC10*, *SLI15*, *STU1*, and *STU2*) affected the localization of either Ase1 or the Esp1–Slk19 complex (Fig. S4, available at http://www.jcb.org/cgi/content/full/jcb.200702145/DC1). With the exception of *IPL1*, *SLI15*, and *NDC10* mutants that impaired Slk19 localization (Pereira and Schiebel, 2003; Norden et al., 2006), we found no defects in the localization of Ase1 and Esp1–Slk19 in any mutant (Fig. S4 and not depicted). This was also the case in the multiple kinesin motor mutant *cin8-3 kip1*Δ *kar3*Δ (Fig. S4; Saunders and Hoyt, 1992). The latter result was surprising because in mammalian cells, PRC1 requires a kinesin motor for correct localization (Kurasawa et al., 2004).

A Cdc14-independent role of Esp1–Slk19 in anaphase spindle formation

Esp1 and Slk19 are part of the Cdc14 early anaphase release network (FEAR) that activates the Cdc14 phosphatase at the beginning of anaphase (Stegmeier et al., 2002). The activated Cdc14 then regulates the spindle localization of Sli15–Ipl1, Cin8, Slk19, and Stu1 (Pereira and Schiebel, 2003; Higuchi and Uhlmann, 2005). The mislocalization of Ase1 in *slk19*Δ or *esp1-1* cells that we report here could therefore arise as an indirect consequence of the failure to activate Cdc14. However, several data argue for a direct function of the Esp1–Slk19 complex in the control of spindle midzone assembly. *pGal1*-induced activation of *CDC14* (Fig. 3) had a marginal impact on the length of the Ase1-GFP spindle domain of *esp1-1* cells, as it only reduced it from 3.1 to 2.5 μm (Fig. 3 C, spindles of 7–8 μm), whereas in *ESP1* WT cells, the Ase1 spindle domain was 1.4 μm long (Fig. S2, spindles of 7–8 μm). Moreover, *pGal1* activation of *CDC14* also had a minimal impact on the mislocalization of Ase1-GFP in *esp1-1* cells (Fig. 3 D). These data demonstrate a direct role of the Esp1–Slk19 complex in Ase1 localization. Consistently, in *ndc10-1* cells, which mislocalize spindle-associated Slk19 (Norden et al., 2006) but release Cdc14 as well as WT cells, Ase1 bound to spindles as in *slk19*Δ cells (unpublished data).

Multiple roles of the phosphatase Cdc14 in anaphase spindle assembly

The spindle midzone localization of Cin8, Slk19, and Stu1 is severely disturbed in *cdc14-2* cells (Pereira and Schiebel, 2003; Higuchi and Uhlmann, 2005). Slk19 mislocalization is caused by the failure of the Sli15–Ipl1 kinase complex to bind to spindle MTs in anaphase. The expression of $SLI15^{6A}$, which binds constitutively to spindle MTs, is therefore partly able to suppress the localization defect of Slk19 in *cdc14-2* cells (Pereira and Schiebel, 2003).

To further analyze the functions of Cdc14 and the Sli15–Ipl1 kinase complex in spindle midzone assembly, we determined the localization of the midzone proteins Ase1, Cin8, Stu1, Bim1, and Esp1 in *cdc14-2* cells with and without the expression of $SLI15^{6A}$. In addition, the role of the Sli15–Ipl1 kinase

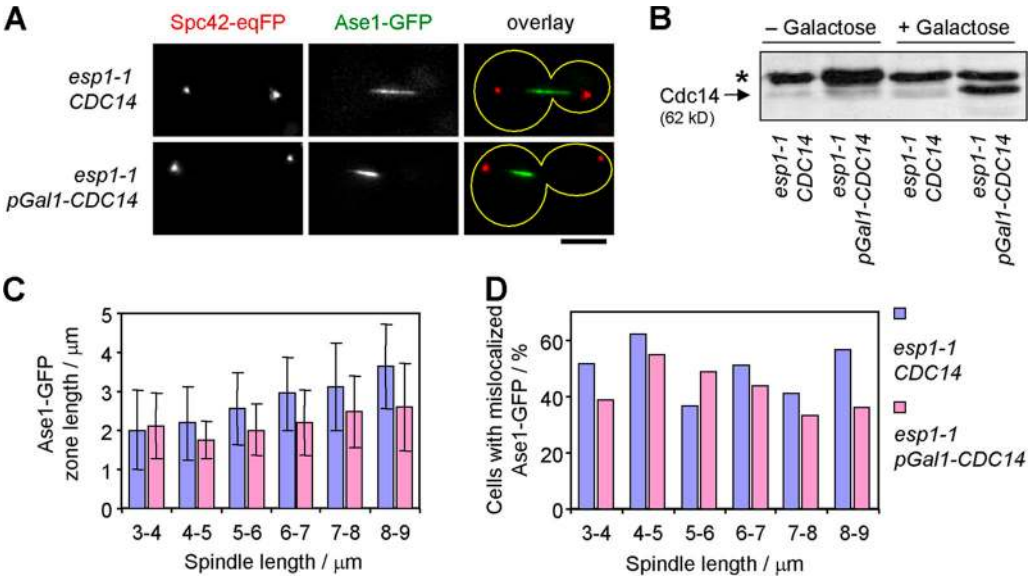

Figure 3. **Regulation of Ase1 localization by Esp1 is independent of Cdc14.** (A) Ase1-GFP localization in *esp1-1 ASE1-GFP SPC42-eqFP* cells with and without the expression of *pGal1-CDC14*. Cells grown in raffinose medium were synchronized with α factor at 23°C in G1 and released into a new cell cycle after removing α actor in the presence of galactose at 37°C. (B) Levels of Cdc14 before (−Gal) and 1 h after induction of the *pGal1* promoter with galactose (+Gal) as determined by immunoblotting with anti-Cdc14 antibodies. The asterisk indicates a protein band that cross reacts with the anti-Cdc14 antibodies. (C and D) Quantification of A. (C) Mean value of the Ase1-GFP zone length with SD (error bars) is shown for each spindle class. (D) Anaphase cells with mislocalized (not centered) Ase1-GFP spindle signal were counted for each spindle class. $n > 30$ per spindle class. Approximate cell morphologies are indicated by yellow outlines drawn onto the overlaid images. Bar, 5 μm.

complex was tested by analyzing the localization of these midzone proteins in conditional lethal *ipl1-321* and *sli15-3* cells.

In *cdc14-2* cells, Esp1 failed to concentrate between the two spindle poles. Instead, Esp1 showed a weak, relatively uniform MT-like staining (Fig. 4 A). This mislocalization of Esp1 was partially rescued by *SLI15*^{6A} (Fig. 4 A), suggesting that the Sli15–Ipl1 pathway regulates Esp1. Consistently, Esp1 failed to bind to spindles in *sli15-3* cells (Fig. 4 A). Thus, Cdc14 regulates Esp1 localization through the Sli15–Ipl1 kinase complex.

In *cdc14-2* cells, Ase1 was either distributed along the entire anaphase spindle (Fig. 4, B, iii; and C, 59%) or the Ase1 zone was shifted toward one spindle pole (Fig. 4, B, ii; and C, 32%). This result was confirmed with temperature-sensitive *cdc14* degron cells (*td-cdc14*; see Fig. 6 D), in which Cdc14 was rapidly degraded upon shifting the cells to the restrictive temperature (Pereira and Schiebel, 2003). To obtain an understanding of whether the regulation of Ase1 was via the Sli15–Ipl1 pathway, we analyzed Ase1 spindle positioning in *cdc14-2 SLI15*^{6A}, *sli15-3* and *ipl1-321* cells. *SLI15*^{6A} was unable to suppress the Ase1 localization defect of *cdc14-2* cells (Fig. 4, B, iv–vi; and C), arguing against a major role for Sli15–Ipl1 in Ase1 regulation. In addition, the defect in Ase1 localization was much stronger in *cdc14-2* than in *sli15-3* or *ipl1-321* cells (Fig. 4, B and C). This suggests that Cdc14 regulates the midzone localization of Ase1. However, contrary to Esp1 and Slk19, the Sli15–Ipl1 complex has little direct influence on Ase1 localization.

Cin8-4GFP, Stu1-4GFP, and Bim1-4GFP localized to spindle MTs in *cdc14-2* cells (Fig. 4 D) but failed to accumulate in the middle of the spindle, as they did in WT cells (Fig. 4 D). The expression of *SLI15*^{6A} in *cdc14-2* cells did not restore the centered localization of Cin8-4GFP, Stu1-4GFP, and Bim1-GFP (Fig. 4 D), suggesting that the Sli15–Ipl1 complex is not directly involved in the targeting of these proteins to the midzone. The finding that in *sli15-3* cells, Cin8-4GFP, Stu1-4GFP, and Bim1-GFP still bound in a spatially restricted manner to the anaphase spindle (Fig. 4 E) reinforced this view. However, in *sli15-3* cells, the Cin8, Stu1, and Bim1 zones were broader than in WT cells and were frequently shifted toward one of the spindle poles (Fig. 4 E). The extent of this defect was comparable with that seen in *slk19*Δ cells (Fig. S3). The defective localization of Slk19 in *sli15-3* cells (Pereira and Schiebel, 2003) is probably responsible for the mislocalization of Cin8, Stu1, and Bim1. Furthermore, the mislocalization of all tested midzone components both in *ase1Δ* and *cdc14-2* mutants and the dependency of Ase1 spindle localization on Cdc14 raises the possibility that Ase1 is a direct target of Cdc14.

Collectively, these data demonstrate that Cdc14 has a dual role in regulating the spindle midzone. Through relocalization of the Sli15–Ipl1 kinase complex, Cdc14 is responsible for midzone targeting of the Esp1–Slk19 complex. In addition, independently of Sli15–Ipl1, Cdc14 is required for the centered and focused localization of other midzone components, possibly by acting on Ase1.

Direct regulation of Ase1 by Cdc14

Ase1 is phosphorylated by Cdk1-Clb5 at the end of S phase, dephosphorylated during anaphase, subsequently targeted for destruction by the anaphase-promoting complex ([APC] APC^{CDH1})/proteasome system during mitotic exit, and reaccumulates again in S phase (Juang et al., 1997; Loog and Morgan, 2005). Moreover, Ase1 is a key protein required for the correct localization of all midzone components (Fig. S3), binds to the

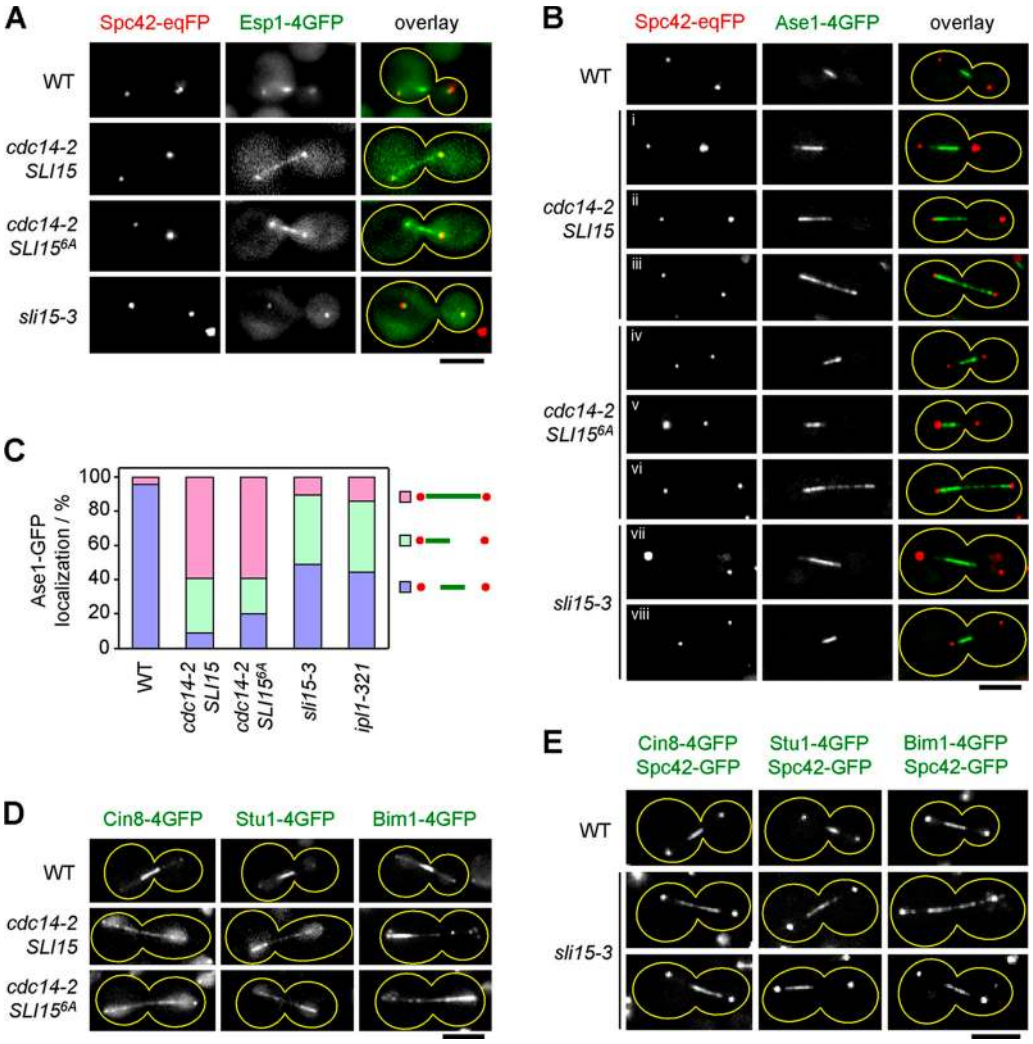

Figure 4. **Multiple roles of Cdc14 in the regulation of anaphase spindle assembly.** (A–E) Localization of spindle midzone proteins in WT, *cdc14-2*, *cdc14-2 SLI15^{6A}*, and *sli15-3* cells. *SPC42-GFP* or *SPC42-eqFP* was used as a marker for SPBs. Cells were synchronized with α factor at 23°C and released into a new cell cycle at 37°C. (A) Localization of Esp1-4GFP in *CDC14 SLI15* (WT), *cdc14-2 SLI15*, *cdc14-2 SLI15^{6A}*, and *CDC14 sli15-3* cells. (B) Ase1-4GFP localization in *CDC14 SLI15* (WT), *cdc14-2 SLI15* (i–iii), *cdc14-2 SLI15^{6A}* (iv–vi), and *CDC14 sli15-3* cells (vii–viii). (C) Quantification of Ase1-4GFP localization in anaphase cells of the indicated types. $n > 200$ for each strain. (D) Localization of 4GFP-tagged Cin8, Stu1, and Bim1 in *CDC14 SLI15* (WT), *cdc14-2 SLI15*, and *cdc14-2 SLI15^{6A}* cells. (E) Localization of 4GFP-tagged Cin8, Stu1, and Bim1 in *SLI15* (WT) and *sli15-3* cells. Approximate cell morphologies are indicated by yellow outlines drawn onto the overlaid images. Bars, 5 μm.

developing midzone before the Esp1–Slk19 centering complex (Fig. 1), and is mislocalized in the *cdc14-2* mutant (Fig. 4). On this basis, we reasoned that Ase1 may be a direct target of Cdc14, allowing the coordination of spindle midzone assembly with anaphase onset. Such a model predicts an interaction between Ase1 and Cdc14. Using the yeast two-hybrid system, we identified an interaction between Ase1 and an N-terminal fragment of Cdc14 (Fig. 5 A).

If Cdc14 dephosphorylates Ase1, we would expect to see an accumulation of hyperphosphorylated Ase1 in cells lacking Cdc14 activity. The phosphorylation of Ase1 was therefore analyzed in α-factor synchronized WT and *td-cdc14* cells (Fig. 5 B). The Ase1-6HA protein accumulated in both cell types around 70 min after release from the G1 block. In *CDC14* and *td-cdc14* cells, a fraction of Ase1-6HA became hyperphosphorylated after ∼80 min, as indicated by the accumulation of slower migrating Ase1 phosphoisoforms (Fig. 5 B, Ase1-P). In WT cells, Ase1-6HA became dephosphorylated and was then degraded with mitotic exit (Clb2 degradation and Sic1 accumulation; Fig. 5 B, 120 min). In contrast, in *td-cdc14* cells, Ase1-6HA remained in the hyperphosphorylated form (Fig. 5 B, 120–150 min). Thus, the dephosphorylation of Ase1 is dependent on Cdc14.

If the proposed model is correct, the premature activation of Cdc14 should dephosphorylate Ase1 at a point in the cell cycle when Cdc14 is normally inactive. This possibility was tested in *pMet3-CDC20 cdc26Δ pGal1-CDC14* and *pMet3-CDC20 cdc26Δ pGal1-CDC14^{C283A}* cells, which lack the APC subunit Cdc26 that is only essential at 37°C (Araki et al., 1992). When grown in the presence of methionine at 37°C, these cells arrested in metaphase without APC activity because of Cdc20 depletion and the absence of Cdc26. In these arrested cells, the endogenous Cdc14 was entrapped in the nucleolus. The *pGal1* promoter was then induced by the addition of galactose, leading

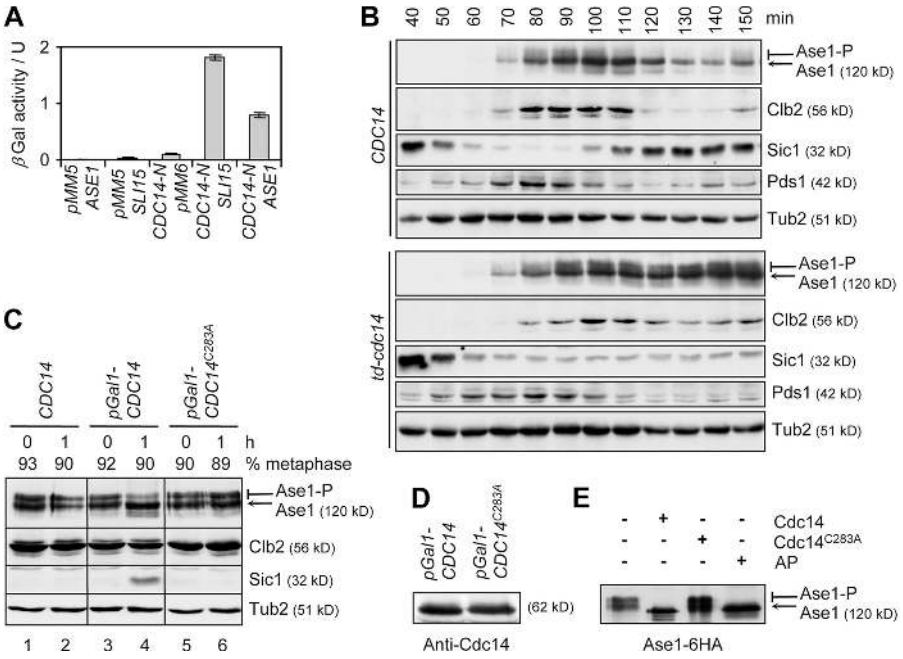

Figure 5. **Cdc14 directly dephosphorylates Ase1.** (A) Ase1 and Cdc14-N interact in the yeast two-hybrid system. Mean values from three independent experiments are shown with SD (error bars). (B) *CDC14 ASE1-6HA* and *td-cdc14 ASE1-6HA* cells were synchronized with α factor in G1 phase (t = 0) at 23°C and released from the block at 37°C (see Materials and methods). Samples were analyzed with the indicated antibodies. (C) *cdc26Δ pMet3-CDC20* cells with *CDC14* (lane 1), *pGal1-CDC14* (lane 3), and *pGal1-CDC14*^{C283A} (lane 5) were arrested in metaphase through Cdc20 depletion (t = 0). Galactose was then added, and the strains were incubated for 1 h at 37°C (lanes 2, 4, and 6). The percentage of metaphase cells was determined for each time point (DAPI staining; $n >$ 100). Samples were analyzed with the indicated antibodies. (D) Cdc14 levels of cells in C (lanes 4 and 6) were similar. (E) Immunoprecipitated Ase1-6HA was incubated with Cdc14, Cdc14^{C283A}, or AP as indicated.

to the accumulation of high levels of Cdc14 or the inactive Cdc14^{C283A} in the nucleus and cytoplasm (Fig. 5 D and not depicted). Despite this accumulation of active Cdc14, cells remained in metaphase (Fig. 5 C, top) mainly because the APC was inactive, and, therefore, Clb2 levels remained high (Fig. 5 C, lane 4). The slight accumulation of the Cdk1 inhibitor Sic1, which was induced by Cdc14 overexpression, was insufficient to promote mitotic exit, as indicated by the failure of cells to rebud or to replicate the DNA (Fig. 5 C; Visintin et al., 1998). Importantly, *pGal1*-activated Cdc14 caused the collapse of most of the hyperphosphorylated Ase1 (Ase1-P) into the nonphosphorylated, faster migrating Ase1 band (Fig. 5 C, lane 4). This was not observed when the phosphatase-dead *CDC14*^{C282A} was expressed (Fig. 5 C, lane 6). Collectively, Cdc14 is responsible for the dephosphorylation of Ase1 in vivo.

Finally, we asked whether recombinant Cdc14 was able to dephosphorylate affinity-purified Ase1 from yeast cells. A first attempt to isolate phosphorylated Ase1 from metaphase-arrested cells failed probably because Cdc14 that was released from the nucleolus during the purification procedure dephosphorylated Ase1 (unpublished data). Hyperphosphorylated Ase1-6HA (Ase1-P) was therefore obtained through immunoprecipitation from arrested *cdc14-2* cells, which lack Cdc14 activity. Enriched Ase1-P was then incubated with buffer only, recombinant Cdc14, the phosphatase-dead Cdc14^{C282A}, or, as a positive control, with AP (Fig. 5 E). Only Cdc14 and AP were able to dephosphorylate Ase1-P, as indicated by the mobility shift. Thus, Cdc14 directly dephosphorylates Ase1.

Dephosphorylation of Ase1 is essential for spindle midzone assembly

Ase1 contains seven Cdk1 consensus sites ([ST]-P-X-[RK]; Fig. 6 A). The serine or threonine residues within these sites were either converted to alanine (*ASE1*^{7A}) to prevent phosphorylation or to aspartic acid (*ASE1*^{7D}) to mimic constitutive phosphorylation. The Ase1^{7A} and Ase1^{7D} proteins no longer showed the mobility shift characteristic for the hyperphosphorylated Ase1 (Fig. 6 B), indicating that most Ase1 phosphorylation sites that were normally responsible for the band shift were blocked.

To understand the relevance of the phosphorylation/dephosphorylation cycle of Ase1, we analyzed the spindle localization of Ase1^{7A} and Ase1^{7D} in *CDC14* and *td-cdc14* cells carrying the SPB marker Spc42-eqFP. In *CDC14* WT cells, the spindle localization of Ase1^{7A}-GFP and Ase1-GFP was similar (Fig. 6, C and D). In contrast, Ase1^{7D}-GFP mislocalized in the majority of *CDC14* WT cells: the Ase1^{7D}-GFP zone either covered large portions of the anaphase spindle or was shifted toward one of the two spindle poles (Fig. 6, C and D). This mislocalization may arise because Ase1^{7D} behaves as a constitutively phosphorylated protein or because the mutations unspecifically affect the function of the protein. In the first case, Ase1 and Ase1^{7D} should show similar localization in *td-cdc14* cells in which Ase1 is hyperphosphorylated (Fig. 5 B). Indeed, in *td-cdc14* cells, Ase1^{7D}-GFP and the hyperphosphorylated Ase1-GFP showed nearly identical localization patterns (Fig. 6 D, *td-cdc14*). Thus, the dephosphorylation of Ase1 is important to assemble a focused spindle midzone.

If the dephosphorylation of Ase1 is an essential step in spindle midzone assembly, Ase1^{7A} should, in part, suppress the spindle defect of *td-cdc14* cells. Indeed, in *td-cdc14* cells, the nonphosphorylated Ase1^{7A}-GFP localized more to the middle of the anaphase spindle than the phosphorylated Ase1-GFP or Ase1^{7D}-GFP (Fig. 6 D, purple area). The failure of Ase1^{7A} to show a WT localization in *td-cdc14* cells is probably the result of the mislocalization of Slk19 in these cells (Pereira and Schiebel, 2003), which, in turn, affects Ase1 localization (Fig. 2 C).

Mislocalization of Ase1^{7D} in *CDC14* cells may affect spindle binding of other midzone proteins. This is expected because the localization of all midzone components depends on *ASE1* (Figs. 2 A and S3). Analysis of Cin8-GFP, Stu1-GFP, and

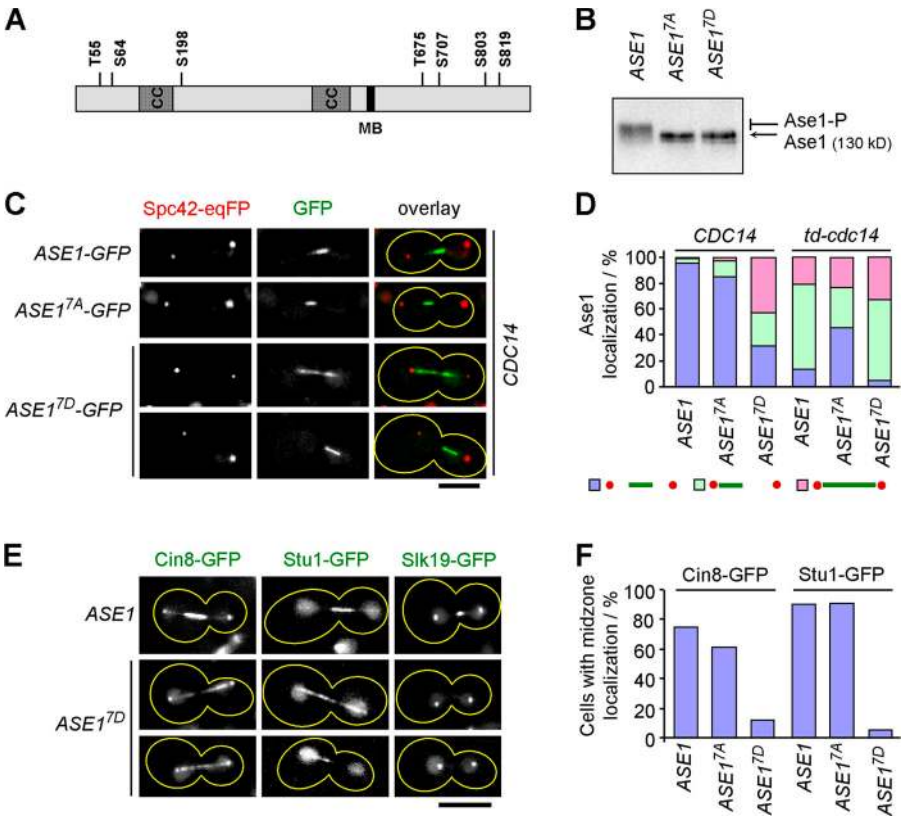

Figure 6. **Dephosphorylation of Ase1 is essential for spindle midzone organization.** (A) Distribution of the seven Cdk1 consensus sites in Ase1. CC, coiled-coil region; MB, MT-binding domain. (B) *td-cdc14* cells expressing *ASE1-GFP*, *ASE1^{7A}-GFP*, or *ASE1^{7D}-GFP* were synchronized with α factor at 23°C and released into a new cell cycle at 37°C. After 3 h of incubation at 37°C, cells were collected and analyzed by immunoblotting with anti-GFP antibodies. (C) Spindle localization of GFP-tagged Ase1, Ase1^{7A}, and Ase1^{7D} in *CDC14* cells. Spc42-eqFP was used as a pole marker. (D) *CDC14* and *td-cdc14* cells with *ASE1-GFP*, *ASE1^{7A}-GFP*, and *ASE1^{7D}-GFP* were grown and synchronized as described in Materials and methods. Spindle localization of Ase1-GFP was quantified as outlined in the figure. $n > 100$ anaphase cells per *CDC14* strain; $n > 500$ anaphase cells per *td-cdc14* strain. (E and F) Localization of Cin8-, Stu1-, and Slk19-GFP in *ASE1*, *ASE1^{7A}*, and *ASE1^{7D}* cells. Cells were grown in YPD at 30°C to mid-log phase. Cells with a single centered GFP domain between the spindle poles were counted as having normal midzone localization. $n > 100$ anaphase cells per strain. Approximate cell morphologies are indicated by yellow outlines drawn onto the overlaid images. Bars, 5 μm.

Slk19-GFP showed that spindle midzone localization of these proteins was severely impaired in *ASE1^{7D}* cells (Fig. 6, E and F). Although Cin8 and Stu1 still bound to the spindle MTs, Slk19 was observed in all *ASE1^{7D}* anaphase cells at the spindle poles but not along the spindle ($n > 100$). Collectively, these data indicate that dephosphorylation of Ase1 by Cdc14 is essential to assemble a focused spindle midzone.

Dephosphorylation of Ase1 is required for continuous extension of the anaphase spindle

Analysis of anaphase B in yeast suggests that the spindle elongates in two phases (Straight et al., 1997). In the first step, the completely overlapping MTs of the metaphase spindle slide apart. This relatively fast elongation is limited to only 1–2 μm. The subsequent slower elongation step of up to 8 μm requires coupling of the sliding of antiparallel MTs with the polymerization of MT plus ends to maintain an overlap zone.

To understand the role of *ASE1* and of a focused midzone in spindle elongation in greater detail, we analyzed the kinetics of anaphase spindle extension of *ASE1*, *ase1*Δ, *ASE1^{7A}*, and *ASE1^{7D}* cells by time-lapse microscopy. The initial fast phase of anaphase spindle extension was identical in all cell types (Fig. 7 A, Table I, and Videos 3–6; available at http://www.jcb.org/cgi/content/full/jcb.200702145/DC1), indicating that Ase1 is not required for this step. Clear differences between WT and the *ASE1* mutants were observed for the second phase. In *ase1*Δ cells, the second extension phase did not occur (Fig. 7 A). *ASE1^{7A}* cells extended the anaphase spindle with close to double the speed of *ASE1* cells (Fig. 7 A and Table I). In addition, in 15% of *ASE1^{7A}* cells, the spindle broke during extension. However, this fracture was not permanent, as the spindle subsequently reformed and extension resumed (Fig. 7 B, t = 9 min; and Video 7, available at http://www.jcb.org/cgi/content/full/jcb.200702145/DC1). Such spindle breakage was not observed in *ASE1* WT cells. *ASE1^{7D}* cells showed a mixed phenotype. 44% of *ASE1^{7D}* cells (12/27) behaved in a manner that was similar to WT cells. This probably reflects the fact that Ase1^{7D} distribution is similar to that of the WT Ase1 molecule in 31% of *ASE1^{7D}* cells (Fig. 6 D). Importantly, in 56% of *ASE1^{7D}* cells (15/27), anaphase spindle extension stalled for up to 10 min after the initial fast phase. After this period of inactivity, the spindle suddenly extended with close to normal speed. The duration of this elongation was reduced, and spindles were shorter than in WT cells (Fig. 7 A and Table I). Thus, a focused spindle midzone is required for processive extension of the anaphase spindle.

ASE1 has an important function in stabilizing the anaphase spindle. This requirement for *ASE1* becomes especially apparent when *cdc15-1* cells are arrested in anaphase (Juang et al., 1997; Sullivan et al., 2001). In 87% of *cdc15-1 ase1*Δ cells that had been arrested for 3 h, the anaphase spindles broke, whereas <18% of *cdc15-1 ASE1* cells showed broken anaphase spindles (Fig. 7 C). Consistent with the spindle breakage that we observed in the time-lapse experiments (Fig. 7 B), a large number of *cdc15-1 ASE1^{7A}* cells had broken anaphase spindles (73% after 3 h). This was in contrast to *ASE1^{7D}* cells, which maintained the anaphase spindle integrity to a similar degree as WT *ASE1* cells (Fig. 7 C). These data suggest that phosphorylation of Ase1 before anaphase onset is important for spindle stability in anaphase.

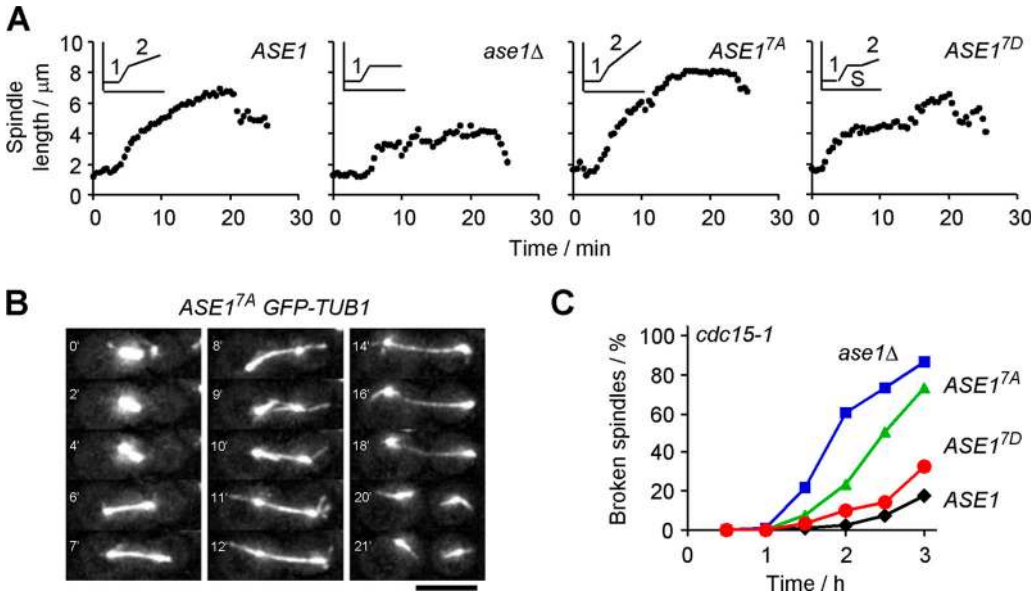

Figure 7. **Dephosphorylation of Ase1 is required for continuous extension of the anaphase spindle.** (A) Kinetics of anaphase spindle extension of *ASE1* WT, *ase1*Δ, *ASE1*^{7A}, and *ASE1*^{7D} cells with *GFP-TUB1* by time-lapse microscopy. Pole to pole distance was measured in three dimensions. Insets depict the different phases of extension: 1, 2, and S (stalled). (B) The spindle breaks during anaphase in *ASE1*^{7A} cells. Selected frames (maximum z-series projections) are shown. Time is indicated in minutes. (C) *cdc15-1 GFP-TUB1* cells with WT *ASE1*, *ase1*Δ, *ASE1*^{7A}, or *ASE1*^{7D} were released from α-factor block and incubated at 37°C (the restrictive temperature). Broken spindles (two half-spindles without continuous GFP-Tub1 signal in between) were scored over time. $n > 100$ spindles per time point. Bar, 5 µm.

Discussion

The midzone is the domain of the spindle that maintains spindle bipolarity during anaphase and generates the forces required for spindle elongation. These functions are provided by midzone proteins that specifically localize to the center of the spindle at the beginning of anaphase (Fig. 1). In this study, we show that the conserved protein phosphatase Cdc14 regulates spindle midzone assembly and function by at least two pathways. Cdc14 directly dephosphorylates Ase1 with anaphase onset and, thereby, triggers spindle midzone assembly. In addition, Cdc14 targets the separase–Slk19 centering complex to the extending anaphase spindle. This complex then positions and concentrates the Ase1 domain in the middle of the anaphase spindle. Thus, activation of Cdc14 with anaphase onset allows coordination of sister chromatid disjunction with the spindle midzone assembly required for anaphase B.

Ase1 and Esp1–Slk19 cooperate to assemble a centered, spatially restricted spindle midzone

Together with fission yeast Ase1, human PRC1, and *C. elegans* SPD-1, budding yeast Ase1 belongs to a group of conserved MT-binding proteins (Schuyler et al., 2003). All Ase1/PRC1-like proteins associate with the spindle midzone and have functions in anaphase spindle formation.

Additional factors involved in spindle midzone assembly in budding yeast include separase Esp1 and its partner Slk19 (Jensen et al., 2001; Sullivan and Uhlmann, 2003). Analysis of the role of Esp1 and Slk19 in spindle function is complicated by the fact that both proteins play critical roles in activation of the anaphase spindle regulator Cdc14 (Stegmeier et al., 2002; Pereira and Schiebel, 2003; Higuchi and Uhlmann, 2005). However, the finding that the *pGal1*-induced activation of Cdc14 only partially reduced the spindle defects of *esp1-1* cells (Fig. 3) supports the view that the Esp1–Slk19 complex has a direct function in midzone assembly.

What are the functions of Ase1 and the Esp1–Slk19 complex in spindle midzone assembly? Ase1 associates with the developing spindle midzone before the Esp1–Slk19 complex (Fig. 1) and is essential to establish a landmark that recruits all other midzone components (Figs. 2 A and S3). The Ase1 landmark develops independently of all other spindle components (Fig. S4), suggesting that it is based on changes of the intrinsic properties of Ase1. Oligomerization of Ase1 with anaphase onset and an increased affinity toward antiparallel MTs, as suggested for human PRC1 and fission yeast Ase1, respectively (Kurasawa et al., 2004; Zhu et al., 2006; Janson et al., 2007), may trigger the self-assembly of Ase1 into a spindle domain.

Human PRC1 binds to the kinesin Kif4, which is then required to localize PRC1 to the spindle midzone (Kurasawa et al., 2004; Zhu et al., 2005). However, kinesin motor proteins do not target Ase1 to the spindle midzone in budding yeast (Fig. S4). Instead, the Esp1–Slk19 complex plays a role in limiting the extent of the Ase1 zone to ~2 µm. Esp1–Slk19 also positions the Ase1 landmark in the middle of the anaphase spindle (Fig. 2 C). The Esp1–Slk19-based system may center the MT overlap zone by destabilizing spindle MTs that exceed a critical length. Such a function was recently proposed for the kinesin-8 Kip3 that has a unique combination of plus end–directed motor and plus end depolymerase activities. These activities of Kip3 at the cell cortex facilitate the positioning of the mitotic spindle

Table I. **Extension speed, extension time, and maximum length of anaphase spindles in *ASE1*, *ase1Δ*, *ASE^{7A}*, or *ASE^{7D}* cells with *GFP-TUB1* analyzed by time-lapse microscopy**

	ASE1	*ase1Δ*	*ASE1^{7A}*	*ASE1^{7D}*		
				WT-like	No phase 2	Phase 2[b]
Phase 1 extension speed (μm/min)	0.94 ± 0.13	0.85 ± 0.13	0.86 ± 0.20	0.83 ± 0.17	0.84 ± 0.28	0.89 ± 0.11
Phase 2 extension speed (μm/min)	0.24 ± 0.04	NA	0.40 ± 0.11	0.19 ± 0.03	NA	0.32 ± 0.09
Stalled phase[a] (duration/min)	NA	NA	NA	NA	13.8 ± 3.3	5.8 ± 2.4
Extension time (min)	17.2 ± 2.4	12.1 ± 4.1	16.2 ± 2.8	16.9 ± 2.3	16.9 ± 3.2	18.8 ± 3.2
Maximum spindle length (μm)	7.2 ± 0.6	4.1 ± 0.9	7.5 ± 0.5	6.3 ± 0.8	4.9 ± 0.4	6.8 ± 0.4

Mean values are indicated with respective SDs. Extension time is defined as the time between the beginning of extension and spindle breakage marked by physical separation of the two half-spindles. Maximum spindle length is defined as the maximum distance between the poles reached during extension. *ASE1*, $n = 10$; *ase1Δ*, $n = 11$; *ASE1^{7A}*, $n = 32$; *ASE1^{7D}*, $n = 27$ (WT-like, $n = 12$; no phase 2, $n = 5$; phase 2, $n = 10$). NA, not applicable.
[a]Phase specific to *ASE1^{7D}* cells; extension is stalled after phase 1.
[b]Resume extension after stalled phase.

(Gupta et al., 2006; Varga et al., 2006) but may also be active at the spindle midzone (Fig. S3; Gupta et al., 2006). However, the observation that *kip3Δ* cells still show normal Ase1 and Slk19 localization argues against such a model (Fig. S4). Alternatively, Ase1 and the Esp1–Slk19 complex may jointly cross-link interdigitating MTs in early anaphase. The assembled Ase1/Esp1–Slk19 domain may then be maintained as cells progress through anaphase. Consistent with this notion is the finding that the length of the Ase1 zone in anaphase is identical to the length of the metaphase spindle (Fig. 2 D).

Cdc14 is a multifunctional regulator of spindle midzone assembly

Recent studies identified Cdc14 as an important regulator of anaphase spindle properties (Pereira and Schiebel, 2003; Higuchi and Uhlmann, 2005; Woodbury and Morgan, 2007). This study pinpoints Cdc14 as a master regulator of the spindle midzone. Cdc14 promotes the assembly and positioning of midzone proteins by acting through at least two pathways: first, directly through Ase1, and second, through regulation of the Esp1–Slk19 centering complex (Fig. 4; Pereira and Schiebel, 2003). Dephosphorylation of Ase1 by Cdc14 is a key event in spindle midzone assembly. In conditional lethal *cdc14* cells or in a large fraction of *CDC14* cells expressing *ASE1^{7D}*, which mimics the constitutive phosphorylated form, Ase1 decorates the entire anaphase spindle in a fairly uniform pattern (Figs. 4 B and 6 C). Other spindle midzone components such as Slk19, Stu1, and Cin8 are also mislocalized in *ASE1^{7D}* cells (Fig. 6 E). The lack of Slk19 at the midzone of *ASE1^{7D}* cells may partly explain the formation of a shifted and unfocused Ase1 landmark.

Spindle midzone assembly is restricted to anaphase through the regulation of Ase1. Before anaphase onset, Ase1 is phosphorylated by Cdk1-Clb5, anaphase completion leads to the APC^{CDH1}-dependent degradation of Ase1 (Juang et al., 1997; Loog and Morgan, 2005). Similar regulatory mechanisms have been described for the spindle-stabilizing protein Fin1 (Woodbury and Morgan, 2007). Cin8 and Kip1 kinesin-like motor proteins, which are required for anaphase spindle extension (Straight et al., 1998), are potentially subject to a similar regulation. Both are Cdk1 substrates (Ubersax et al., 2003) and become degraded with mitotic exit by an APC^{CDH1}-dependent mechanism (Hildebrandt and Hoyt, 2001; Crasta et al., 2006). Dephosphorylation by Cdc14 regulates the MT binding of Sli15 (Pereira and Schiebel, 2003) and MT stabilization by the DASH component Ask1 (Higuchi and Uhlmann, 2005). Thus, Cdc14-mediated dephosphorylation seems to be an efficient way to promote the quick changes in MT organization and behavior observed at anaphase onset.

The Cdc14 regulation of the Esp1–Slk19 centering system is much less understood, but it requires the Aurora B kinase complex. Dephosphorylation of the inner centromere protein subunit by Cdc14 targets the Aurora B kinase complex to spindle MTs at the beginning of anaphase (Pereira and Schiebel, 2003). Aurora B then recruits the Esp1–Slk19 complex via an unknown mechanism to the spindle midzone (Fig. 4; Pereira and Schiebel, 2003). However, this is only part of the story because the kinetochore component Ndc10, which associates with spindles in complex with the Aurora B kinase subunit survivin, is also required for binding of the Esp1–Slk19 complex to anaphase spindles (Bouck and Bloom, 2005; Norden et al., 2006; unpublished data). In addition, Ndc10 localization to spindle MTs also requires Cdc14 activity (Bouck and Bloom, 2005). Presently, it is unclear how Ndc10 and survivin cooperate with Esp1–Slk19.

Consequences of the regulation of Ase1 by Cdc14

How does the phosphorylation and dephosphorylation of Ase1 regulate the properties of the anaphase spindle? Analysis of the mutated Ase1^{7A} protein that lacks all Cdk1 consensus phosphorylation sites and of Ase1^{7D} in which these consensus sites have been switched to acidic residues to mimic the hyperphosphorylated state of Ase1 provided an answer to this question. The vast majority of *ASE1^{7A}* cells assembled a proper spindle midzone (Fig. 6 D). A more detailed analysis of this mutant revealed that *ASE1^{7A}* cells extended their anaphase spindle faster

than *ASE1* WT cells (Fig. 7 A and Table I). In addition, the spindle of *ASE1*^{7A} cells frequently broke during anaphase B. This breakage phenotype was accentuated by prolonged cell cycle arrest in late anaphase (Fig. 7, B and C). The reason for this malfunction is presently unclear, but it may arise from the hyperactivation of motor proteins that drive anaphase spindle extension. Such hyperactive motors would interfere with the coordination of polymerization, antiparallel sliding, and cross-linking of MTs that is an integral part of spindle extension in anaphase B and could, therefore, prevent the attenuation of spindle extension at the end of anaphase (Table I).

The majority of *ASE1*^{7D} cells failed to assemble a focused or centered spindle midzone (Fig. 6 D). Instead, the Ase1^{7D} protein was frequently spread along the spindle. This phenotype allowed us to analyze the importance of a focused spindle midzone. Surprisingly, the dephosphorylation of Ase1 was not important for the initial fast phase of anaphase B (Fig. 7 A and Table I) or for spindle stability (Fig. 7 C). The close to WT stability of anaphase spindles of *ASE1*^{7D} cells was intriguing because the stabilizing protein Slk19 was no longer associated with the interpolar MTs in this mutant (Fig. 6 E). The most prominent defect of *ASE1*^{7D} cells was a delay in the slower phase of anaphase B (Fig. 7 A and Table I), which requires coupling between the sliding of antiparallel MTs and the polymerization of MT plus ends (Straight et al., 1997). This delayed extension of the anaphase spindle in *ASE1*^{7D} cells may compensate for the lack of Slk19 at the spindle midzone. Thus, a focused Ase1 zone is likely to be important for the coordination of polymerization and sliding of MTs in anaphase B but not for spindle stability.

Conserved feature of the Ase1/PRC1 family

Analysis of spindle midzone assembly in yeast has shown that even this relatively simple organism possesses an elaborate system to mediate and control the assembly of a centered spindle midzone. The requirement for Ase1 and its regulation by cell cycle–dependent dephosphorylation are clearly conserved features of spindle midzone assembly (Juang et al., 1997; Mollinari et al., 2002; Loiodice et al., 2005; Zhu et al., 2006). In yeast, the protein phosphatase Cdc14 directly dephosphorylates Ase1. CeCDC-14 also has been implicated in spindle midzone formation in *C. elegans* (Gruneberg et al., 2002). Moreover, PRC1 dephosphorylation is required for spindle midzone formation (Zhu et al., 2006). Whether SPD-1 and PRC1 are regulated by the *C. elegans* and human Cdc14 orthologues remains to be addressed.

Our analysis has also shown differences regarding the Ase1/PRC1 centering systems. One distinction is the lack of the requirement for kinesin motors for the focusing of Ase1. The larger size of the human metaphase spindle (10 μm) probably demands the active transport of PRC1 to MT plus ends with anaphase onset. It is currently unclear how the established spindle midzone of mammalian spindles remains centered between the two spindle poles. This control must influence the plus end properties of MTs according to the position of their ends within the anaphase spindle. It will be interesting to see whether such a system reflects or is an extension of the scheme seen in yeast.

Materials and methods

Strain constructions and growth conditions

Gene deletions and epitope tagging of genes at their endogenous loci were performed using PCR-based methods (Janke et al., 2004). *td-stu1* cells were constructed and grown as described previously (Kanemaki et al., 2003). The strains and plasmids used in this study are listed in Table S1 (available at http://www.jcb.org/cgi/content/full/jcb.200702145/DC1). All yeast strains were derivatives of S228c with the exception of *esp1-1 mcd1-1 mad1*Δ (referred to as *esp1-1* in the text and figures), which was derived from W303 and was compared with the corresponding WT, K699.

Typically, cells were grown in yeast extract peptone glucose medium (YPD) at 23°C and shifted to 30°C or the restrictive temperature for 3 h before observation. For synchronization, cells were incubated with 10 μg/ml of synthetic α factor for 2.5–3 h at 23°C until >95% of cells were in G1 phase. After washing with prewarmed medium to remove α factor, cells progressed synchronously through the cell cycle. Cells were arrested in metaphase by depletion of *CDC20* under control of the *pMet3* promoter by incubating the cells for 3–4 h in yeast extract peptone raffinose (YPR) medium supplemented with 2 mM methionine and 2 mM cysteine until >95% of cells were with a large bud. The APC was inactivated by incubating arrested *pMet3-CDC20 cdc26*Δ metaphase cells at 37°C. *CDC14* and *CDC14*^{C283A} were expressed from the *pGal1* promoter cloned into yeast integration plasmids. The *pGal1* promoter was induced by the addition of 2% galactose to the grow medium. *ESP1-GFP* was expressed from the native promoter cloned into the yeast integration plasmid pRS406.

Construction of *ASE1* mutants

ASE1 with regulatory and coding regions was cloned into the yeast integration vector pRS306. Mutations in *ASE1* were introduced by PCR-directed mutagenesis and confirmed by DNA sequencing. Serine or threonine residues of seven Cdk1 consensus sites ([ST]-P-X-[KR]) were mutated to alanine to avoid phosphorylation or mutated to aspartic acid to mimic phosphorylation (Fig. 6 A). The *ASE1*^{7A} mutant resulted from the exchange of threonine 55, serine 64, serine 198, threonine 676, serine 707, serine 803, and serine 819 to alanine. In *ASE1*^{7D}, the same set of amino acids was exchanged to aspartic acid.

Yeast two hybrid

ASE1, *SLI15*, and *CDC14-N* (N-terminal fragment; amino acids 1–352) were cloned into pMM5 and pMM6 vectors. Interaction between Sli15 and Cdc14-N was used as a positive control (Pereira and Schiebel, 2003). Two-hybrid interactions were tested as described previously (Schramm et al., 2000).

Dephosphorylation of Ase1 by Cdc14

For in vitro dephosphorylation assay, Ase1-6HA was immunoprecipitated from a *cdc14-2 ASE1-6HA* cell extract. Immunoprecipitates were incubated with buffer, maltose-binding protein–Cdc14, or maltose-binding protein–Cdc14^{C283A} (both purified from *Escherichia coli*) for 1 h at 30°C as described previously (Pereira and Schiebel, 2003). Proteins were analyzed by immunoblotting with anti-HA antibodies.

Antibodies and immunoblotting

Yeast extracts were prepared using alkaline lysis and TCA precipitation (Janke et al., 2004). Anti-Cdc14 (6His-Cdc14), anti-Clb2 (GST-CLB2$^{1–271}$), anti-GFP (GST-GFP), anti-Pds1 (GST-Pds1$^{1–173}$), and anti-Tub2 antibodies (GST-Tub2$^{436–457}$) were prepared in rabbits or sheep against purified recombinant proteins (Pereira and Schiebel, 2003). Monoclonal mouse anti-myc (9E10) and anti-HA (12CA5) antibodies were purchased from Roche, and guinea pig anti-Sic1 antibodies were a gift from G. Pereira (German Cancer Research Centre, Heidelberg, Germany).

Fluorescence microscopy

For live cell imaging (Figs. 1 and 7), cells were adhered with concanavalin A on small glass-bottom Petri dishes (MatTek). Imaging was performed at 30°C on a microscope (DeltaVision RT; Applied Precision) equipped with GFP and TRITC filters (Chroma Technology Corp.), a plan Apo 100× NA 1.4 oil immersion objective (IX70; Olympus), softWoRx software (Applied Precision), and a camera (CoolSNAP HQ; Photometrics). Measurements were performed using softWoRx software and complete z stacks.

Still images of nonfixed cells in growth medium were acquired at room temperature with a wide-field epifluorescence microscope (Axio Imager.A1; Carl Zeiss MicroImaging, Inc.) equipped with a plan-Fluar

100× NA 1.45 oil immersion objective (Carl Zeiss MicroImaging, Inc.), a camera (Cascade:1K; Photometrics), and MetaMorph software (Universal Imaging Corp.). Quantification was performed using MetaMorph software and complete z stacks. Photoshop (Adobe) was used to mount the images and to produce merged color images. No manipulations other than contrast, brightness, and color balance adjustments were used. Approximate cell morphologies are indicated by yellow outlines drawn onto the overlaid images.

Online supplemental material

Fig. S1 shows the spindle binding of Ase1 relative to Bim1 and Slk19 by analysis of still images of synchronized cells. Fig. S2 shows interdependency of the midzone localization of Ase1, Esp1, and Slk19. Fig. S3 shows the localization of spindle proteins in *ase1*Δ and *slk19*Δ cells. Fig. S4 shows Ase1 localization in spindle mutants. Table S1 lists strains and plasmids used in this study. Video 1 shows the spindle localization of Ase1 relative to Slk19 in an *ASE1-GFP SLK19-tdTomato* cell corresponding to Fig. 1 A. Video 2 shows spindle localization of Ase1 relative to Bim1 in an *ASE1-GFP BIM1-eqFP* cell corresponding to Fig. 1 B. Videos 3–6 show spindle extension in *ASE1*, *ase1*Δ, *ASE1^{7A}*, and *ASE1^{7D}* cells corresponding to Fig. 7 A, respectively. Video 7 shows spindle breakage during extension in an *ASE1^{7A}* cell corresponding to Fig. 7 B. Online supplemental material is available at http://www.jcb.org/cgi/content/full/jcb.200702145/DC1.

We thank A. Hoyt, T. Hyman, and A. Amon for yeast strains, J. Pines and M. Knop for plasmids, G. Pereira for antibodies, I. Hagan and members of the Schiebel laboratory for comments on the manuscript, and U. Jäkle for technical assistance.

This work was supported by Marie Curie Training Network grants to A. Khmelinskii and J. Roostalu. The work of C. Lawrence was funded by Cancer Research UK.

Submitted: 21 February 2007
Accepted: 16 May 2007

References

Araki, H., K. Awane, N. Ogawa, and Y. Oshima. 1992. The *CDC26* gene of *Saccharomyces cerevisiae* is required for cell growth only at high temperature. *Mol. Gen. Genet.* 231:329–331.

Balasubramanian, M.K., E. Bi, and M. Glotzer. 2004. Comparative analysis of cytokinesis in budding yeast, fission yeast and animal cells. *Curr. Biol.* 14:R806–R818.

Belmont, L.D., A.A. Hyman, K.E. Sawin, and T.J. Mitchison. 1990. Real-time visualization of cell cycle-dependent changes in microtubule dynamics in cytoplasmic extracts. *Cell*. 62:579–589.

Berlin, V., C.A. Styles, and G.R. Fink. 1990. BIK1, a protein required for microtubule function during mating and mitosis in *Saccharomyces cerevisiae*, colocalizes with tubulin. *J. Cell Biol.* 111:2573–2586.

Bouck, D.C., and K.S. Bloom. 2005. The kinetochore protein Ndc10p is required for spindle stability and cytokinesis in yeast. *Proc. Natl. Acad. Sci. USA*. 102:5408–5413.

Carazo-Salas, R.E., G. Guarguaglini, O.J. Gruss, A. Segref, E. Karsenti, and I.W. Mattaj. 1999. Generation of GTP-bound Ran by RCC1 is required for chromatin-induced mitotic spindle formation. *Nature*. 400:178–181.

Cassimeris, L., C.L. Rieder, and E.D. Salmon. 1994. Microtubule assembly and kinetochore directional instability in vertebrate monopolar spindles: implications for the mechanism of chromosome congression. *J. Cell Sci.* 107:285–297.

Chan, J., C.G. Jensen, L.C. Jensen, M. Bush, and C.W. Lloyd. 1999. The 65-kDa carrot microtubule-associated protein forms regularly arranged filamentous cross-bridges between microtubules. *Proc. Natl. Acad. Sci. USA*. 96:14931–14936.

Cooke, C.A., M.M. Heck, and W.C. Earnshaw. 1987. The inner centromere protein (INCENP) antigens: movement from inner centromere to midbody during mitosis. *J. Cell Biol.* 105:2053–2067.

Crasta, K., P. Huang, G. Morgan, M. Winey, and U. Surana. 2006. Cdk1 regulates centrosome separation by restraining proteolysis of microtubule-associated proteins. *EMBO J.* 25:2551–2563.

DeZwaan, T.M., E. Ellingson, D. Pellman, and D.M. Roof. 1997. Kinesin-related KIP3 of *Saccharomyces cerevisiae* is required for a distinct step in nuclear migration. *J. Cell Biol.* 138:1023–1040.

Gruneberg, U., M. Glotzer, A. Gartner, and E.A. Nigg. 2002. The CeCDC-14 phosphatase is required for cytokinesis in the *Caenorhabditis elegans* embryo. *J. Cell Biol.* 158:901–914.

Gupta, M.L., Jr, P. Carvalho, D.M. Roof, and D. Pellman. 2006. Plus end-specific depolymerase activity of Kip3, a kinesin-8 protein, explains its role in positioning the yeast mitotic spindle. *Nat. Cell Biol*. 8:913–923.

Higuchi, T., and F. Uhlmann. 2005. Stabilization of microtubule dynamics at anaphase onset promotes chromosome segregation. *Nature*. 433:171–176.

Hildebrandt, E.R., and M.A. Hoyt. 2001. Cell cycle-dependent degradation of the *Saccharomyces cerevisiae* spindle motor Cin8p requires APC(Cdh1) and a bipartite destruction sequence. *Mol. Biol. Cell*. 12:3402–3416.

Janke, C., M.M. Magiera, N. Rathfelder, C. Taxis, S. Reber, H. Maekawa, A. Moreno-Borchart, G. Doenges, E. Schwob, E. Schiebel, and M. Knop. 2004. A versatile toolbox for PCR-based tagging of yeast genes: new fluorescent proteins, more markers and promoter substitution cassettes. *Yeast*. 21:947–962.

Janson, M.E., R. Loughlin, I. Loiodice, C. Fu, D. Brunner, F. Nedelec, and P.T. Tran. 2007. Crosslinkers and motors organize dynamic microtubules to form stable bipolar arrays in fission yeast. *Cell*. 128:357–368.

Jensen, S., M. Segal, D.J. Clarke, and S.I. Reed. 2001. A novel role of the budding yeast separin Esp1 in anaphase spindle elongation: evidence that proper spindle association of Esp1p is regulated by Pds1p. *J. Cell Biol.* 152:27–40.

Jiang, W., G. Jimenez, N.J. Wells, T.J. Hope, G.M. Wahl, T. Hunter, and R. Fukunaga. 1998. PRC1: a human mitotic spindle-associated CDK substrate protein required for cytokinesis. *Mol. Cell*. 2:877–885.

Jin, Q.-w., E. Trelles-Sticken, H. Scherthan, and J. Loidl. 1998. Yeast nuclei display prominent centromere clustering that is reduced in nondividing cells and in meiotic prophase. *J. Cell Biol.* 141:21–29.

Juang, Y.-L., J. Huang, J.-M. Peters, M.E. McLeughlin, C.-Y. Tai, and D. Pellman. 1997. APC-mediated proteolysis of Ase1 and the morphogenesis of the mitotic spindle. *Science*. 275:1311–1314.

Kanemaki, M., A. Sanchez-Diaz, A. Gambus, and K. Labib. 2003. Functional proteomics by induced proteolysis in vivo identifies novel DNA-replication proteins. *Nature*. 423:720–724.

Kurasawa, Y., W.C. Earnshaw, Y. Mochizuki, N. Dohmae, and K. Todokoro. 2004. Essential roles of KIF4 and its binding partner PRC1 in organized spindle midzone formation. *EMBO J.* 23:3237–3248.

Loiodice, I., J. Staub, T.G. Setty, N.-P.T. Nguyen, A. Paoletti, and P.T. Tran. 2005. Ase1p organizes antiparallel microtubule arrays during interphase and mitosis in fission yeast. *Mol. Biol. Cell*. 16:1756–1768.

Loog, M., and D.O. Morgan. 2005. Cyclin specificity in the phosphorylation of cyclin-dependent kinase substrates. *Nature*. 434:104–108.

Mallavarapu, A., K. Sawin, and T. Mitchison. 1999. A switch in microtubule dynamics at the onset of anaphase B in the mitotic spindle of *Schizosaccharomyces pombe*. *Curr. Biol.* 9:1423–1428.

Mollinari, C., J.-P. Kleman, W. Jiang, G. Schoehn, T. Hunter, and R.L. Margolis. 2002. PRC1 is a microtubule binding and bundling protein essential to maintain the mitotic spindle midzone. *J. Cell Biol.* 157:1175–1186.

Norden, C., M. Mendoza, J. Dobbelaere, C.V. Kotwaliwale, S. Biggins, and Y. Barral. 2006. The NoCut pathway links completion of cytokinesis to spindle midzone function to prevent chromosome breakage. *Cell*. 125:85–98.

Pereira, G., and E. Schiebel. 2003. Separase regulates INCENP-Aurora B anaphase spindle function through Cdc14. *Science*. 302:2120–2124.

Saunders, W.S., and M.A. Hoyt. 1992. Kinesin-related proteins required for structural integrity of the mitotic spindle. *Cell*. 70:451–458.

Schramm, C., S. Elliott, A. Shevchenko, A. Shevchenko, and E. Schiebel. 2000. The Bbp1p-Mps2p complex connects the SPB to the nuclear envelope and is essential for SPB duplication. *EMBO J.* 19:421–433.

Schuyler, S.C., J.Y. Liu, and D. Pellman. 2003. The molecular function of Ase1p: evidence for a MAP-dependent midzone-specific spindle matrix. *J. Cell Biol.* 160:517–528.

Schwartz, K., K. Richards, and D. Botstein. 1997. *BIM1* encodes a microtubule-binding protein in yeast. *Mol. Biol. Cell*. 8:2677–2691.

Stegmeier, F., R. Visintin, and A. Amon. 2002. Separase, polo kinase, the kinetochore protein Slk19, and Spo12 function in a network that controls Cdc14 localization during early anaphase. *Cell*. 108:207–220.

Straight, A.F., W.F. Marschall, J.W. Sedat, and A.W. Murray. 1997. Mitosis in living budding yeast: anaphase A but no metaphase plate. *Science*. 277:574–578.

Straight, A.F., J.W. Sedat, and A.W. Murray. 1998. Time-lapse microscopy reveals unique roles for kinesins during anaphase in budding yeast. *J. Cell Biol.* 143:687–694.

Sullivan, M., and F. Uhlmann. 2003. A non-proteolytic function of separase links the onset of anaphase to mitotic exit. *Nat. Cell Biol.* 5:249–254.

Sullivan, M., C. Lehane, and F. Uhlmann. 2001. Orchestrating anaphase and mitotic exit: separase cleavage and localization of Slk19. *Nat. Cell Biol.* 3:771–777.

Ubersax, J.A., E.L. Woodbury, P.N. Quang, M. Paraz, J.D. Blethrow, K. Shah, K.M. Shokat, and D.O. Morgan. 2003. Targets of the cyclin-dependent kinase Cdk1. *Nature*. 425:859–864.

Varga, V., J. Helenius, K. Tanaka, A.A. Hyman, T.U. Tanaka, and J. Howard. 2006. Yeast kinesin-8 depolymerizes microtubules in a length-dependent manner. *Nat. Cell Biol.* 8:957–962.

Verbrugghe, K.J., and J.G. White. 2004. SPD-1 is required for the formation of the spindle midzone but is not essential for the completion of cytokinesis in *C. elegans* embryos. *Curr. Biol.* 14:1755–1760.

Verde, F., J.-C. Labbe, M. Doree, and E. Karsenti. 1990. Regulation of microtubule dynamics by cdc2 protein kinase in cell-free extracts of *Xenopus* eggs. *Nature*. 343:233–238.

Verni, F., M.P. Somma, K.C. Gunsalus, S. Bonaccorsi, G. Belloni, M.L. Goldberg, and M. Gatti. 2004. Feo, the *Drosophila* homolog of PRC1, is required for central-spindle formation and cytokinesis. *Curr. Biol.* 14:1569–1575.

Visintin, R., K. Craig, E.S. Hwang, S. Prinz, M. Tyers, and A. Amon. 1998. The phosphatase Cdc14 triggers mitotic exit by reversal of Cdk-dependent phosphorylation. *Mol. Cell*. 2:709–718.

Wiedenmann, J., A. Schenk, C. Röcker, A. Girod, K.-D. Spindler, and G.U. Nienhaus. 2002. A far-red fluorescent protein with fast maturation and reduced oligomerization tendency from *Entacmaea quadricolor* (Anthozoa, Actinaria). *Proc. Natl. Acad. Sci. USA*. 99:11646–11651.

Woodbury, E.L., and D.O. Morgan. 2007. Cdk and APC activities limit the spindle-stabilizing function of Fin1 to anaphase. *Nat. Cell Biol.* 9:106–112.

Yamashita, A., M. Sato, A. Fujita, M. Yamamoto, and T. Toda. 2005. The roles of fission yeast Ase1 in mitotic cell division, meiotic nuclear oscillation, and cytokinesis checkpoint signalling. *Mol. Biol. Cell*. 16:1378–1395.

Yin, H., L. You, D. Pasqualone, K.M. Kopski, and T.C. Huffaker. 2002. Stu1p is physically associated with beta-tubulin and is required for structural integrity of the mitotic spindle. *Mol. Biol. Cell*. 13:1881–1892.

Zeng, X., J.A. Kahana, P.A. Silver, M.K. Morphew, J.R. McIntosh, I.T. Fitch, J. Carbon, and W.S. Saunders. 1999. Slk19p is a centromere protein that functions to stabilize mitotic spindles. *J. Cell Biol.* 146:415–425.

Zhu, C., J. Zhao, M. Bibikova, J.D. Leverson, E. Bossy-Wetzel, J.B. Fan, R.T. Abraham, and W. Jiang. 2005. Functional analysis of human microtubule-based motor proteins, the kinesins and dyneins, in mitosis/cytokinesis using RNA interference. *Mol. Biol. Cell*. 16:3187–3199.

Zhu, C., E. Leu, R. Schwarzenbacher, E. Bossy-Wetzel, and W. Jiang. 2006. Spatiotemporal control of spindle midzone formation by PRC1 in human cells. *Proc. Natl. Acad. Sci. USA*. 103:6196–6201.